

AD-A121 174

INVESTIGATIONS OF TURBULENT NATURAL CONVECTION IN A  
HORIZONTAL CYLINDER(U) CLEMSON UNIV SC DEPT OF  
MECHANICAL ENGINEERING J A LIBURDY JUL 82

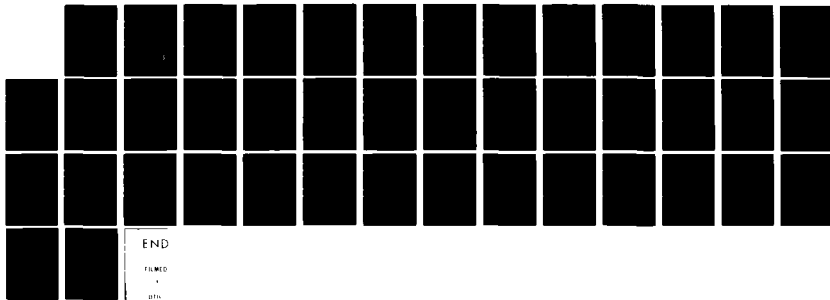
1/1

UNCLASSIFIED

AFOSR-TR-82-0956 AFOSR-80-0181

F/G 28/4.

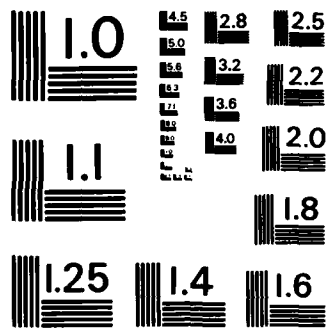
NL



END

ENMED

0116



MICROCOPY RESOLUTION TEST CHART  
NATIONAL BUREAU OF STANDARDS - 1963 - A

ADA121174

AFOSR-TR- 82-0956

(12)

FINAL REPORT

AFOSR  
80-0181

May 1980 - May 1982

INVESTIGATIONS OF TURBULENT  
NATURAL CONVECTION IN A  
HORIZONTAL CYLINDER

by

James A. Liburdy

Mechanical Engineering Department

Clemson University

Clemson, SC 29631

DTIC  
ELECTED  
S NOV 8 1982 D  
B

Project Monitor:

Dr. James Wilson

USAF Office of Scientific Research

Bolling Air Force Base, DC 20332

DISTRIBUTION STATEMENT A

Approved for public release;  
Distribution Unlimited

32 11 08 005

## SUMMARY

This document presents results of an experimental investigation of natural convection within a horizontal cylinder subjected to a constant wall heat flux. The work was completed under USAF Office of Scientific Research Grant 80-0181 monitored by Dr. James Wilson. The studies were carried out from May 1, 1980 to May 15, 1982 at the Thermal Science Laboratory of the Mechanical Engineering Department at Clemson University, South Carolina.

The nature of transient natural convection heat transfer within a horizontal cylinder was studied. Results of the mean and local wall heat transfer coefficients scale in terms of the parameter ( $FoRa^*$ ) where  $Fo$  is the Fourier modulus and  $Ra^*$  a modified Rayleigh number based on the wall heat flux. A Nusselt-Rayleigh number correlation for water is found to be  $Nu = 1.09(Ra^*)^{.195}$ . The temperature distribution, measured along the horizontal and vertical diameters, show a slight stratification and distinct side wall thermal boundary layer development. A fine wire thermocouple probe sensed the temperature fluctuations, and indicates turbulence levels to be related to  $Ra^*$ , relative wall position, and confined to a thin boundary layer region. The central core recirculation pattern consists of two large cells with mixing zones, possibly three dimension, near the top and bottom of the cylinder.

AIR FORCE OFFICE OF SCIENTIFIC RESEARCH (AFSC)  
NOTICE OF TRANSMITTAL TO DTIC  
This technical report has been reviewed and is  
approved for public release IAN AFR 190-12.  
Distribution is unlimited.  
MATTHEW J. KERPER  
Chief, Technical Information Division

## TABLE OF CONTENTS

	<u>Page</u>
Summary .....	i
Table of Contents .....	ii
Nomenclature .....	iii
Introduction .....	1
Experimental Apparatus and Procedure .....	4
Results and Discussion .....	8
Conclusions .....	15
References .....	16
Publications and Paper Presentations .....	20
List of Figures .....	21

Accession No.	
Ref ID:	<input checked="" type="checkbox"/>
Printed:	<input type="checkbox"/>
Unpublished:	<input type="checkbox"/>
Justified:	<input type="checkbox"/>
By _____	
Distribution / _____	
Availability Codes	
Dist	Avail and/or Special
A	



## NOMENCLATURE

$C_p$  - specific heat

$D$  - cylinder diameter

$F_o$  - Fourier modulus =  $\frac{\alpha}{r_o^2}$

$G_r$  - Grashof number =  $\frac{g\beta D^3 \Delta T}{v^2}$

$G_r^*$  - modified Grashof number =  $\frac{g\beta D^4 q''}{kv^2}$

$h$  - local wall film coefficient

$\bar{h}$  - average wall film coefficient

$k$  - fluid thermal conductivity

$L$  - cylinder length

$N_u$  - Nusselt number =  $hD/k$

$Pr$  - Prandtl number =  $v/\alpha$

$q''$  - wall heat flux into fluid

$Q$  - wall heat transfer into fluid

$r$  - radial coordinate

$r_o$  - cylinder radius

$R_a$  - Rayleigh number

$R_a^*$  - modified Rayleigh number =  $Gr^*Pr$

$t$  - time

$T_w$  - wall temperature

$T_w$  - average wall temperature

$\Delta T$  - temperature difference =  $T_w - T_b$

$\bar{\Delta T}$  - average temperature difference =  $T_w - T_b$

$\Delta T_b$  - difference between ideal and actual bulk and fluid temperature, see

Eq. (6)

V - volume

#### Greek Letters

$\alpha$  - thermal diffusivity

$\beta$  - volumetric thermal expansion coefficient

$\rho$  - density

$\theta$  - circumferential coordinate =  $0^\circ$  at bottom of cylinder

$\nu$  - kinematic fluid viscosity

#### Subscripts

b - bulk fluid temperature

e - property of the end plates

f - fluid property

i - evaluated at initial conditions

l - local wall value

ss - quasi-steady state value

w - wall value

## INTRODUCTION

Investigations are made as to the transient nature of turbulent natural convective heat transfer inside a horizontal cylinder. This particular geometry has been studied previously, however, with the main objectives being the steady state mean Nusselt number correlations as influenced by the boundary conditions. This study involves time dependent property variations for a liquid when the cylinder wall is subjected to a constant uniform heat flux. Such a situation may occur during heating or cooling of chemical storage containers, thermal storage mediums, etc.

The problem of identifying a relevant heat transfer coefficient is compounded by the temperature dependence of the fluid's thermal properties. Thus gases and liquids might be expected to behave differently under identical boundary conditions. The goal of this investigation is to identify the transient behavior of the local and averaged nondimensional parameters relating the heat transfer coefficient with the applied heat flux. A representation is given for water which relates the Nusselt number to a modified Rayleigh number evaluated at the initial conditions. Thermal structure is identified in the core and boundary layer regions. Some qualitative flow field data is related to the thermal conditions. Discussion is also given on the effect of end heat losses from the cylinder.

Apparently Maahs [1] in 1964 was the first to study a similar problem of a uniformly heated fluid in a horizontal cylinder. He correlated a Nusselt number with Rayleigh number based on the wall-bulk fluid temperature difference. A transient correlation was presented in terms of the Fourier modulus,  $Fo = (ta/r^2)$ . A quasi-steady state condition was identified when the wall-fluid temperature difference became constant with time.

Deaver and Eckert [2] using a liquid filled horizontal cylinder varied the uniform wall temperature at a steady rate. They present a quasi-steady state Nusselt number - Rayleigh number correlation where fluid properties are evaluated at the quasi-steady state condition. Another transient study of horizontal and vertical fluid filled cylinders was reported by Evans and Stefany [3]. They applied a sudden uniform step change of wall temperature and found a constant convection film coefficient after a short initial conduction period. Their Nusselt-Rayleigh number correlation is based on the initial step change in temperature and properties evaluated at the wall temperature.

Transient convection in a rectangular enclosure was investigated numerically by Aziz and Hellums [4]. They indicate the time dependent nature of the Nusselt number not taking into account property variations of the dimensionless variables. Nusselt number when mapped against the Fourier modulus shows an initial rise, a peak and a slight decrease toward a steady state value. Their results are for low Ra (maximum = 3800). The time required to reach steady state increases as Ra increases or Pr increases, however, they began each new case from the steady state solution of the previous case.

Steady state investigations of natural convection inside cylinders have been conducted by numerous authors. The boundary conditions have basically consisted of a heat source and a heat sink imposed on the cylinder wall. Ostrach and co-workers, both experimentally [5,6] and analytically [7,8,9] studied the variation of the heat source-sink distribution on the temperature and velocity profiles within the cylinders. It appears that the boundary conditions can influence the core structure and boundary layer development along the side walls. Weinbaum [10] analytically studied a similar problem. Leong

and deVahl Davis [11] show that the Nu-Ra correlation, based on numerical approximations of the governing equations, is dependent on the temperature boundary condition distribution around the periphery.

The question arises, for the constant heat flux condition, how one can evaluate an appropriate Nusselt and Rayleigh number for convenient application. A true steady state is never achieved during the heating or cooling process since fluid properties are continually changing. Also, the use of a wall-fluid temperature difference to define the Rayleigh number is inappropriate since it is not known apriori. This temperature difference is not readily measurable because of relatively large peripheral wall temperature variations coupled with the difficulty of determining the fluid temperature.

The transition to turbulence and its effects on the overall heat transfer correlations has not been reported in the literature for the geometry and conditions of concern in this investigation. Kuehn and Goldstein [12] have described a transition to turbulent boundary layer flow for the annular gap between concentric horizontal cylinders to occur near a Rayleigh number of  $10^7$  based on the gap thickness. Their conclusion is drawn from interferogram observations.

The nature of the enclosed flow supposes that the existence of a core cellular structure may interact with side boundary layer flow. Measurements by Brooks and Ostrach [6] suggest a narrow boundary layer regime existing near the cylinder walls. The local Reynolds number based on the boundary layer thickness may become very large at large Rayleigh numbers suggesting that local turbulence, near the walls, may exist.

## EXPERIMENTAL APPARATUS AND PROCEDURE

The experimental apparatus consisted of a water filled cylinder oriented horizontally subjected to a constant, uniform wall heat flux. Measurements included the transient bulk fluid temperature, local fluid temperatures and local wall temperatures. A schematic of the experimental apparatus is shown in Figure 1. The cylinder, made from aluminum, was .18m inside diameter, .32m long, and mounted with two vertical supports which could be adjusted to assure a horizontal orientation of the central axis. The inside surface was machined and polished smooth, the wall thickness being 9.5mm. Welded flanges at either end were used to secure 6.3mm thick plate glass windows held in place by a double "O"-ring seal.

Heating was accomplished with a uniform electrical resistance wrap around heater that fit the entire outside surface area. Power supplied to the heater was monitored with a multimeter to measure voltage and current. During a run the power input was continuously monitored to assure consistency. Energy supplied by the heater went to heating the cylinder and its supports, heating the insulation, heating the fluid, and some was lost by conduction through the supports and convection to the environment. The energy supplied to the fluid varied from 64% to 75% of the total energy generated with the lower input percentage occurring during the low heat flux case. The energy supplied to the fluid was measured from the fluid expansion described below.

Wall temperature measurements were made with sixteen type J thermocouples embedded in the wall to within 1.5mm of the inner wall surface. A high thermal conductivity paste was used to assure good thermal contact. Eight thermocouples were situated at 45° intervals around the midplane. Four

thermocouples were arranged at 90° intervals two-thirds of the distance away from the midplane towards either end. Thus circumferential and axial wall temperature variations were detected. All thermocouple generated voltages were recorded with a 40 channel datalogger. The datalogger was programmed to sample all sensors at preset intervals whereby all temperatures could be recorded within 15 seconds. The data logger also served as an accurate clock.

The bulk fluid temperature was determined by measuring the fluid expansion in a vertically adjustable standpipe. The standpipe position was continuously adjusted to maintain a constant pressure condition inside the cylinder. This was done using a long translation screw to position the standpipe which was mounted on a moveable platform. This was found necessary due to expansion of the cylinder end plates under increased pressure loading. The vertical displacement was measured to  $\pm 0.025\text{mm}$ , this is equivalent to  $\pm 0.005^\circ\text{C}$  at  $38^\circ\text{C}$  for the 25.4mm diameter standpipe. Correction was made for the thermal expansion of the aluminum cylinder using a constant thermal expansion coefficient. The expansion coefficient for water was evaluated at the instantaneous bulk fluid temperature. The total uncertainty of the change of the bulk fluid temperature due to expansion measurements, cylinder temperature measurements and the measurement of the cylinder volume was determined to be approximately  $\pm 2^\circ\text{C}$ .

A thermocouple probe was used to determine the temperature distribution across the midplane of the cylinder. The probe was mounted on a steel arc which surrounded the cylinder but was not in contact with it. Figure 1 shows the mounting positions. The probe could be moved to various circumferential positions to allow radial and circumferential measurements. A feed through port was made to allow the probe to traverse radially without leaking fluid.

When the probe was not mounted over any port a sealing plug was used which was machined smooth with the inside wall. A rack and pinion arrangement with a dial indicator was used to position the sensor relative to the cylinder inside wall. The probe could be positioned to within  $\pm .5$ mm. The probe itself was a 1.6mm outside diameter stainless steel tube, the portion inside the cylinder was bent at slightly greater than  $90^\circ$ . This minimized interruption of the convection currents by providing radial entry of the probe approximately 6.5cm from the midplane. The thermocouple sensor (0.3mm diameter iron-constantan junction) was epoxied so it protruded from the tip of the steel tube approximately 1mm. The thermocouple time constant was less than approximately 50 milliseconds.

Each run began by completely filling the cylinder and standpipe with distilled, deairated water. The water-cylinder system was then allowed to come to thermal equilibrium and the initial temperatures of the wall recorded. The initial fluid temperature was then taken to be uniformly equal to the wall temperature. This was checked using the thermocouple probe by measuring the center fluid temperature. The heater was then turned on to a preset power level. All wall temperatures and the fluid expansion were measured at set time intervals. As the run proceeded the standpipe was vertically adjusted to assure a constant fluid level referenced to a fixed point on the cylinder. Heating continued until the fluid temperatures approached the boiling point. Depending on the applied heat flux runs typically lasted two to five hours. Table 1 lists the test conditions of the runs. Many runs were made at each applied heat flux to assure repeatability, however, only the data set for one run at each heat flux level is presented. Variations of the measured wall and bulk fluid temperatures for runs at the same heat flux level were less than 2%.

TABLE 1 Test Conditions

Test Run	T <sub>initial</sub> °C	T <sub>final</sub> °C	Q <sub>input</sub>	R <sub>a*</sub> <sub>i,ss</sub>	R <sub>a</sub> <sub>ss</sub>
A	24.5	87.6	123.7	1.97x10	1.13x10
B	26.6	87.1	168.4	2.93x10	1.20x10
C	23.7	87.4	248.3	3.61x10	1.67x10
D	22.6	88.8	343.6	4.71x10	2.04x10
E	26.1	89.0	415.8	6.84x10	2.42x10

Both local and wall averaged heat transfer coefficients were calculated. The wall averaged values were based on the average wall temperature minus the bulk fluid temperature. All sixteen wall embedded thermocouples were used in the averaging process. The arrangement of the thermocouples were such that each represented an equal wall surface area.

Flow visualization studies were undertaken in both air and water filled cylinders. The cylinder was constructed by joining two aluminum cylinders between a plexiglass ring which formed a 1 cm wide window to view the midplane. A laser sheet was passed through the window to illuminate the flow. For air, smoke was slowly injected into a small port at the bottom of the cylinder at the midplane to provide the scattering sites to view the flow. Glass end plates allowed viewing.

In water the visualization was accomplished by injecting 1  $\mu\text{m}$  diameter latex particles which were neutrally buoyant. The particles were injected through a 1 mm I.D. tube positioned at the cylinder bottom. The flow field was front lighted and streaklines observed.

## RESULTS AND DISCUSSION

A dimensional analysis of natural convection inside an enclosure using the heat flux as a parameter yields the following relationship

$$Nu = f(Gr, \frac{q''D}{\Delta T R}, Pr, Fo, L/D) \quad (1)$$

Terms are defined in the Nomenclature where  $Gr$ ,  $Pr$ , and  $Fo$  have the usual definitions. The Grashof number and the second parameter in Equation (1) can be combined to form a modified Grashof number  $Gr^*$  which eliminates the  $\Delta T$  dependence. Other nondimensional groups have been deleted from those listed in Equation (1). These are  $\beta T$  and  $\Delta T/T_b$  which have been shown to be of minor influence on the function  $f$  for the test conditions studied [10 and 14].

The data reported herein is restricted to one fluid as such Prandtl number effects are not isolated. Thus  $Gr^*$  and  $Pr$  are combined to form a modified Rayleigh number,  $Ra^*$ . Since  $L/D$  effects are not uniquely studied Equation (1) can be reduced to

$$Nu = f_1(Ra^*, Fo) \quad (2)$$

If a quasi-steady state condition can be defined for this problem then one might expect Equation (2) to be further reduced to

$$Nu_{ss} = f_2(Ra^*)$$

where  $Nu_{ss}$  represents a type of steady state value. Equation (3) however, is further complicated by the fact that fluid properties are continually changing with time. As heating (or cooling) is induced property changes result in a significant increase (or decrease) of  $Ra^*$  for most liquids. Meanwhile  $Nu$  will increase at a different rate as the bulk fluid temperature rises. For the tests conducted  $Ra^*$  varied by approximately a factor of 10 during a given run.

The instantaneous value of  $Nu$  was determined using the following relationship:

$$Nu = \frac{D^2}{4\alpha\Delta T} \frac{dT_b}{dt} \quad (4)$$

To obtain the wall average Nusselt number  $\Delta T$  is replaced by  $\bar{\Delta T}$ . The time derivative of the bulk fluid temperature was evaluated by polynomial curve fitting the transient fluid temperature data.  $T_b$  is essentially linear for the high heat flux cases except for an initial thermal lag. At lower heat flux levels the time rate change of  $T_b$  decreases slightly with time, similarly for the average wall temperatures,  $T_w$ . In all cases a unique third order polynomial using a least-squares fit matched all the data points to less than 0.5 percent for a given run.

The nonlinearity of the bulk fluid temperature rise with time is caused by end effects. During peripheral heating of the cylinder walls the end plates experience a time dependent inside boundary condition related to the bulk fluid temperature. To determine the relative effects of conduction loss out the ends a one dimensional analysis of transient conduction in a semi-infinite wall was carried out. The insulation used at the ends was

sufficiently thick to lend itself to this type of analysis which is further validated by virtue of the fact that no detectable temperature rise was noticed at the outside surface of the insulation. For the analysis a lumped capacitance model was used which included an end loss term. A constant value of  $h$  was assumed but it is felt that this will have little effect on the conclusions since only relative effects are of importance. With these constraints the bulk fluid temperature can be expressed as a combination of a linear time dependence, an exponential term due to the initial thermal lag between wall and fluid and a time dependent end loss term. The details are given in the Appendix, the resulting equation is

$$T - T_i = \frac{C_2}{C_1^2} [C_1 t + e^{-C_1 t} - C_3 t^{3/2}] \quad (5)$$

where  $C_1$ ,  $C_2$ , and  $C_3$  are constants defined in the Appendix. The last term represents the end loss and is based on the assumption of a linear time dependent inside boundary condition of the end plate surface temperature. As shown in the Appendix the relative difference of the bulk temperature, with and without loss,  $\Delta T_b$ , compared to the actual wall-bulk fluid temperature difference,  $\Delta T$ , is:

$$\frac{\Delta T_b}{\Delta T} = \frac{8}{3\sqrt{\pi}} \frac{D}{L} \frac{k_e}{k_D} \sqrt{\frac{\alpha_b}{\alpha_e}} \text{Nu} F_o^{3/2} \quad (6)$$

where  $\Delta T_b = T_{b,ideal} - T_{b,actual}$ . In the early stages of heating losses are relatively unimportant but increase rapidly with the  $3/2$  power of  $Fo$ . The effect is also dependent on the heating rate through  $Nu$ .

A correction can be made to the measured data by assuming a linear  $T_b$  versus time relationship or by calculating  $T_b$  from Equation (6). The

versus time relationship or by calculating  $T_b$  from Equation (6). The latter would be an iterative process because of the Nu dependence. The former assumes negligible loss in the early part of a run and projects the rate of energy gain by the fluid to later times.

Figure 2 shows the variation of the temperature difference measured for each run versus time. In Figure 2.a it can be seen that an apparent constant  $\bar{\Delta}T$  is approached for each run with longer times associated with lower heat flux levels. Figure 2.b attempts to appropriately stretch the time scale by taking into account the applied heat flux using  $Ra^*$ . For the range of the  $Ra^*$  investigated a constant  $\bar{\Delta}T$  condition is achieved for  $FoRa^* > 10^9$ . The trend seems to indicate that  $FoRa^*$  at the quasi-steady state conditions may increase as  $Ra^*$  increases. Note that each run experiences a slight dip below the final  $\bar{\Delta}T$  value. It is felt this is caused by thermal lag between the fluid and wall as each responds to the energy loss from the ends of the cylinder discussed previously. As the fluid experiences a greater relative loss of energy the bulk fluid temperature will no longer be linear with time, and the  $T_b$  versus time plot will show a downward curvature. Similarly  $T_w$  versus time will also show a similar response, however, at a slightly later time. Thus at some point there will be a minimum value of  $\bar{\Delta}T$ . This will result in a maximum value of Nu.

The transient nature of the local Nusselt number,  $Nu_\lambda$ , is shown in Figure 3 for runs A and E. Plotted are the values for the bottom, side and top positions,  $0=0, 90^\circ$  and  $180^\circ$  respectively. Larger values occur at the bottom of the cylinder because of the lower local wall temperature - this is shown in Figure 4. Significant transient variations occur at the bottom and side portions of the cylinder while the top region appears less varient. This indicates larger relative changes of the local wall temperature on the lower portion of the cylinder wall.

Figure 4 gives the circumferential wall temperature variation at the quasisteady state condition. All profiles during other times of the runs exhibited a similar shape. Much higher values occur at the top of the cylinder and the lowest values at the cylinder bottom. This would indicate poorer circulation in the upper region compared to the lower portion of the cylinder.

Qualitative flow visualization studies revealed some correlating effects between the velocity field and the local heat transfer coefficient. Studies in air showed two primary cell formations symmetric about the vertical centerline. Mixing zones at the top and bottom appeared to be three dimensional. The cell rotation was such that upward boundary layer type flow existed at both side walls. During the transient heating the flow field remained essential constant and was well established very early.

Flow patterns observed in water were somewhat different than in air. A decidedly thinner boundary layer appeared near the side walls. A more stagnant central core existed and the inner cellular structure was not as obvious. Mixing zones did exist at the upper and lower regions.

At the quasi-steady state condition the circumferential variation of the local Nusselt number is shown in Figure 5. The percent variation from the mean value is rather significant and is highest for the lower heat flux cases. This is because of the rather low values of  $\bar{\Delta}T$ . The heat transfer coefficients near the lower portion of the cylinder are enhanced by the induced fluid motion caused by a downward facing plume along the vertical centerline.

The fluid temperature distribution along the vertical centerline is shown in Figure 6.a and along the horizontal radius in Figure 6.b. The temperature field appears somewhat stratified in the central core region indicative of strong mixing. Significant upper and lower thermal boundary layer type condi-

tions exist. Across the horizontal radial the fluid is increasingly hotter towards the wall. The near linear variation indicates ineffective horizontal mixing to better unify the temperature distribution. There does appear to be a rather narrow thermal boundary layer region near the wall.

As indicated previously a quasi-steady state condition may be defined as when  $\Delta T$  approaches a constant value. By stretching the Fourier modulus with  $Ra^*$  a near single value was found for  $FoRa^*$  for quasi-steady state. Similarly the average Nusselt number can be so represented. In order to accommodate the problem of continuous  $Nu$  variation caused by property changes it was decided to evaluate properties at the initial temperature and thus define  $Nu_i$ . Similarly ( $FoRa^*$ ) is the stretched time scale whose properties are evaluated at the initial temperature. Figure 7.a and 7.b show the instantaneous and initial temperature property evaluation of this correlation. As can be seen in Figure 7.b the quasi-steady state condition for  $Nu_i$  occurs at values of  $(FoRa^*)_i$  greater than  $2 \times 10^9$ . The greater energy loss associated with the lower heat flux runs is reflected in a larger relative peak  $Nu_i$ .

Based on the results indicated in Figure 7.b a  $Nu_{i,ss}$  versus  $Ra_i^*$  correlation can be formulated, where the subscript ss represents the quasi-steady state condition. Figure 8 shows the corrected data and the correlation equation

$$Nu_{i,ss} = 1.09 (Ra_i^*)^{1.94} \quad (7)$$

This equation is based on a least squares linear regression of the data. All data points fall within  $\pm 5\%$  of this correlating equation. The data was corrected for end losses by assuming a linear time-bulk temperature relation-

ship derived from the initial 70 to 80 percent of the data per run. In so doing the loss term effect in Equation (5) is minimized. All the bulk temperature data, neglecting the final points, fell to within 0.5 percent of the values predicted by the linear curve fit.

In order to compare these results with previous investigations it is necessary to form a Rayleigh number based on  $\Delta T$  such as used by Maahs [1] and Deaver and Eckert [2]. This is inconvenient and normally not obtainable in practice when attempting to predict  $Nu$  for an applied heat flux. Choosing the  $\overline{\Delta T}$  at steady state conditions  $Nu_{ss}$  versus  $Ra$  is shown in Figure 9 along with the correlation of Maahs. The data is shown for both the corrected and uncorrected cases. Notice that the correction is essentially zero for the high heat flux case and is approximately 17 percent for the low heat flux case. The corrected correlation is best fitted with the following

$$Nu_{ss} = 0.34 Ra^{.27} \quad (8)$$

as compared to Maahs' correlation of  $Nu_{ss} = 1.215 Ra^{.21}$ . All corrected data points are within 4 percent of Maahs' correlation, the differences between the two correlations may be caused by a limited number of data points in the present study.

Figure 10 shows traces of the thermocouple probe output at three circumferential positions, two radial positions, and three test conditions. The scale is such that 1 cm of horizontal travel represents 20 seconds and 1 cm of vertical displacement represents  $^{\circ}\text{C}$ . At  $\theta = 0^{\circ}$ , bottom position, near the wall,  $r/r_o = .96$  a definite increase in fluctuating intensity is noted for higher Rayleigh numbers. Near wall and far wall fluctuations appear to have nearly

the same amplitude but the near wall fluctuations are decidedly more frequent.

Highest intensities occur at the side wall,  $\theta = 90^\circ$ . The highest frequencies were approximately 0.25 cps at  $r/r_o = .96$  for run D. At  $r/r_o = 8$  for the same run the frequency drops to 0.08 cps. Virtually no fluctuations were recorded near the top of the cylinder for all runs.

One can surmise from these results that the energy input from the walls, which generates the boundary layer type flow, becomes turbulent in nature but quickly decays toward the more structured large cellular motion and mixing regions that exist in center, upper and lower parts of the cylinder cross section.

#### CONCLUSIONS

Natural convection of liquid within a horizontal cylinder with a uniform, constant wall heat flux results in substantial transient and peripheral variation of the Nusselt number. A modified Rayleigh number can be used to correlate the heat transfer data where properties are evaluated at the initial conditions at least for the range of parameters studied in this investigation.

The time to reach a quasi-steady state value is a function of  $FoRa^*$ . End effects can play a major role in influencing the heat transfer correlations and must be adequately accounted for in any empirical relationships.

#### REFERENCES

1. Maahs, H. G., "Transient Natural Convection Heat Transfer in a Horizontal Cylinder," Ph.D. Thesis, Univ. of Washington, 1964.
2. Deaver, F. and Eckert, E., "An Interferometric Investigation of Convective Heat Transfer in a Horizontal Fluid Cylinder with Wall Temperature Increasing at a Uniform Rate," in Heat Transfer 1970, Vol. 4, Elsevier Publishing Co., Amsterdam, 1970.
3. Evans, L. and Stefany, N., "An Experimental Study of Transient Heat Transfer to Liquids in Cylindrical Enclosures," Chem. Engr. Prog. Symp. Series, Vol. 62, 1966, pp. 209-213.
4. Aziz, K. and Hellums, D., "Numerical Solution of the Three Dimensional Equations of Motion for Laminar Natural Convection," The Physics of Fluids, Vol. 10, No. 2, 1967, pp. 314-324.
5. Sabzervani, A. and Ostrach, S., "Experimental Studies of Natural Convection in a Horizontal Cylinder," AFOSR, Sci. Rep. No. 66-1401 (1966).
6. Brooks, I., and Ostrach, S., "An Experimental Investigation of Natural Convection in a Horizontal Cylinder," Journal of Fluid Mechanics, Vol. 44, 1970, pp. 545-561.
7. Menald, E. and Ostrach, S., "Natural Convection in a Horizontal Cylinder at Large Prandtl Numbers," AFOSR, Tech. Rep. No. 65-2239, 1965.
8. Ostrach, S., "Natural Convection in Enclosures," Advanced in Heat Transfer 1972, ed. Harnett, J. P. and Irvine, T. F., Academic Press, New York, 1972.
9. Martini, W. and Churchill, S., "Natural Convection Inside a Horizontal Cylinder," A.I.Ch.E. Journal, Vol. 6, No. 2, 1960, pp. 251-257.

10. Weinbaum, S., "Natural Convection in a Horizontal Cylinder," Journal of Fluid Mechanics, Vol. 18, 1964, pp. 409-437.
11. Leong, S. and deVahl Davis, G., "Natural Convection in a Horizontal Cylinder," Proceedings of the First International Conference, University College, Swansea, July 2-6, 1979, Pineridge Press, Swansea, UK, 1979, pp. 287-296.
12. Evans, L. B., Reid, R. C., and Drake, E. M., "Transient Natural Convection in a Vertical Cylinder," A.I.Ch.E. Journal, Vol. 14, No. 2, 1968, pp. 251-255.
13. Hess, C. F. and Miller, C. W., "Natural Convection in a Vertical Cylinder Subject to a Constant Heat Flux," Int. J. Heat Mass Transfer, Vol. 22, 1979, pp. 421-443.
14. Clausing, A. M. and Kempka, S. N., "The Influences of Property Variations on Natural Convection from Vertical Surfaces," J. Heat Transfer, Vol. 103, No. 4, 1981, pp. 609-612.

#### APPENDIX

A lumped capacitance model is used to determine the time dependence of the end loss effect on the bulk fluid temperature. The system consists of the fluid, cylinder wall, and end plates. The governing equations derived from an energy balance on the system are:

$$(\rho C_p V)_b \frac{dT_b}{dt} = hA(T_w - T_b) - \dot{Q}_e(t) \quad (A.1)$$

$$(\rho C_p V)_w \frac{dT_w}{dt} = \dot{Q} - hA(T_w - T_b) \quad (A.2)$$

where  $Q_e(t)$  is the heat loss out the ends and  $Q$  is the energy input to the system. Initially at  $t=0$  the values of  $T_b$  and  $T_w$  equal  $T_i$  (the initial temperature), and by virtue of Equation (A.1)  $\frac{dT_b}{dt} = 0$  at  $t=0$ .

These equations can be combined to form a single differential equation:

$$T_b(D^2 - D(K_w + K_b)) - K_e(t) = 0 \quad (A.3)$$

$$\text{where } K_w = \frac{hA}{(\rho CpV)}_w$$

$$K_b = \frac{hA}{(\rho CpV)}_b$$

and  $D$  represents the differential operator with respect to time.

Equation (A.3) once integrated yields:

$$T_b(D + C_1) - C_1 T_i - F(t) = 0 \quad (A.4)$$

where  $F(t) = \int_0^t K_e(t)dt$  and  $C_1 = K_w t K_b$ . The general solution to Equation (A.4) is

$$e^{C_1 t} T_b = \int_0^t e^{C_1 T} F(t)dt + C_0 \quad (A.5)$$

Equation (A.5) is evaluated assuming a linear end plate inner surface temperature rise with time which is related to the bulk temperature rise which in turn is related to the applied heat flux. The result is

$$T_b = T_i + \frac{C_2}{C_1^2} [C_1 t + e^{-C_1 t-1}] - C_3 t^{3/2} \quad (A.6)$$

where  $C_2 = \frac{4Qh}{(\rho CpV)_w (\rho CpD)_b}$

and  $C_3 = \frac{4Q\alpha e}{3(\rho CpV)_b^2} \frac{ke}{\sqrt{\pi\alpha e}}$

The subscript e refers to the end plates. It has been assumed, in evaluating  $C_3$ , that  $(\rho C_p V)_w$  is much less than  $(\rho C_p V)_b$ . In the experiments of this study  $(\rho C_p V)_w$  was approximately 7 percent of  $(\rho C_p V)_b$ .

The last term of Equation (A.6) represents end loss effects in reducing the bulk fluid temperature. The exponential term is the initial thermal lag between the wall and fluid. In our experiments this term becomes negligible during the first few minutes of a run.

We can formulate a nondimensional end loss parameter which is the ratio of the reduction of the bulk fluid temperature from the ideal case to the actual wall-fluid temperature difference:

$$\frac{\Delta T_b}{\Delta T} = \frac{8}{3\sqrt{\pi}} \frac{D}{L} \frac{k_e}{k_D} \sqrt{\frac{\alpha_b}{\alpha_e}} \quad \text{Nu} \text{ Fo}^{3/2} \quad (\text{A.7})$$

where Nu and Fo are defined in the Nomenclature, and  $\Delta T_b = T_b, \text{ideal} - T_b, \text{actual}$ . This analysis then assumes that the reduction of the bulk fluid temperature due to end losses is independent of variations of h which should be valid near latter times in the experiments as a quasi-steady state condition is reached.

## PUBLICATIONS AND PAPER PRESENTATIONS

Results of the investigations described in this final report have been reported in

- (1) "Transient Natural Convection in a Horizontal Cylinder with Constant Heat Flux" by Z. Hugue, Master's of Science Thesis, Mechanical Engineering Department, Clemson University, Clemson, S.C.
- (2) "Natural Convection in a Horizontal Cylinder with Constant Heat Flux" by Z. Hugue and J. A. Liburdy, to be presented at the 1982 ASME Winter Annual Meeting, Phoenix, AZ, Nov. 1982.

## LIST OF FIGURES

- Figure 1. (a) Side view of Experimental apparatus  
(b) End view of Experimental apparatus
- Figure 2. (a) Temperature - time plot for each run using the nondimensional time,  $F_o = \frac{at}{r_o^2}$   
(b) Temperature - time plot for each run using the stretch time scale  $F_o Ra^*$
- Figure 3. Local Nusselt number versus Fourier modulus for runs A and E.
- Figure 4. Circumferential variation of the nondimensional wall temperature at the quasi-steady state condition
- Figure 5. Circumferential variation of the local Nusselt number
- Figure 6. (a) Nondimensional fluid temperature distribution along the vertical diameter  
(b) Nondimensional fluid temperature distribution along the horizontal radius
- Figure 7. (a) Nusselt number versus the time scale  $F_o Ra^*$  at the quasi-steady state condition  
(b) Nusselt number versus the time scale  $F_o Ra^*$  at the quasi-steady state condition where all properties are evaluated at the initial condition
- Figure 8. Nusselt number versus modified Rayleigh number correlation where properties are evaluated at the initial condition
- Figure 9. Nusselt number versus Rayleigh number correlation
- Figure 10. Temperature fluctuation indications at three circumferential positions, and two radial positions for three heat flux values

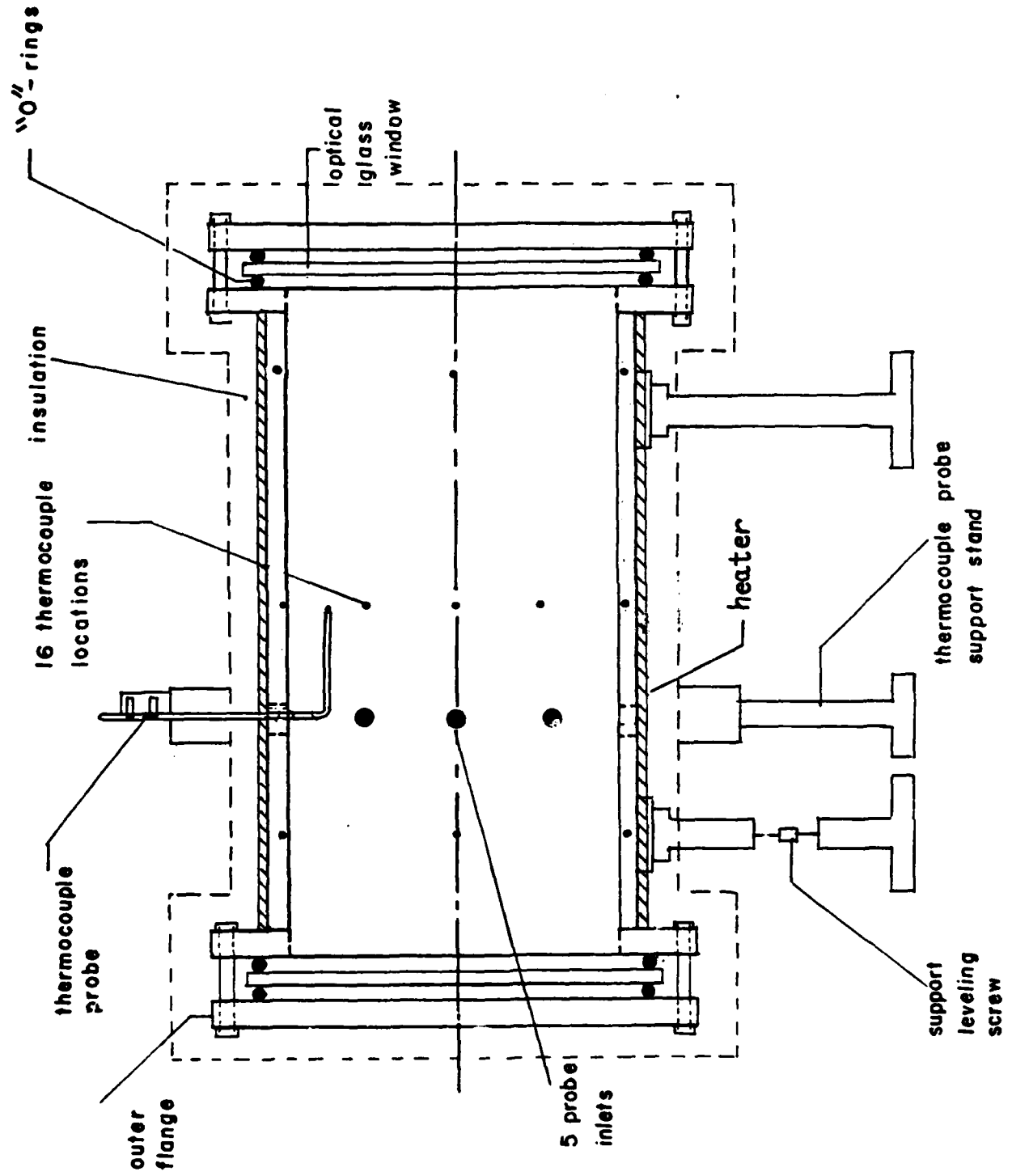


FIGURE 1. (a)

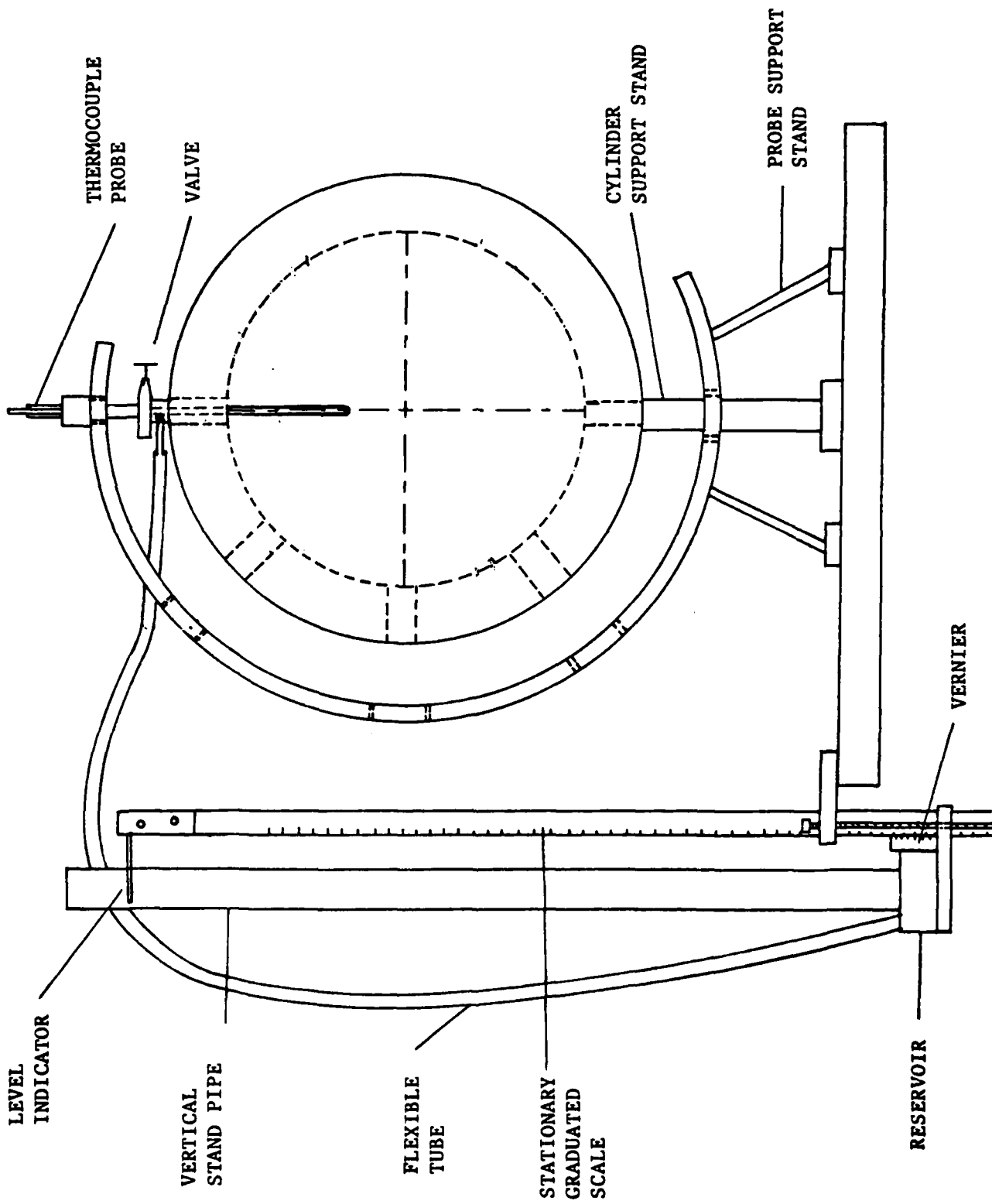


FIGURE 1.(b)

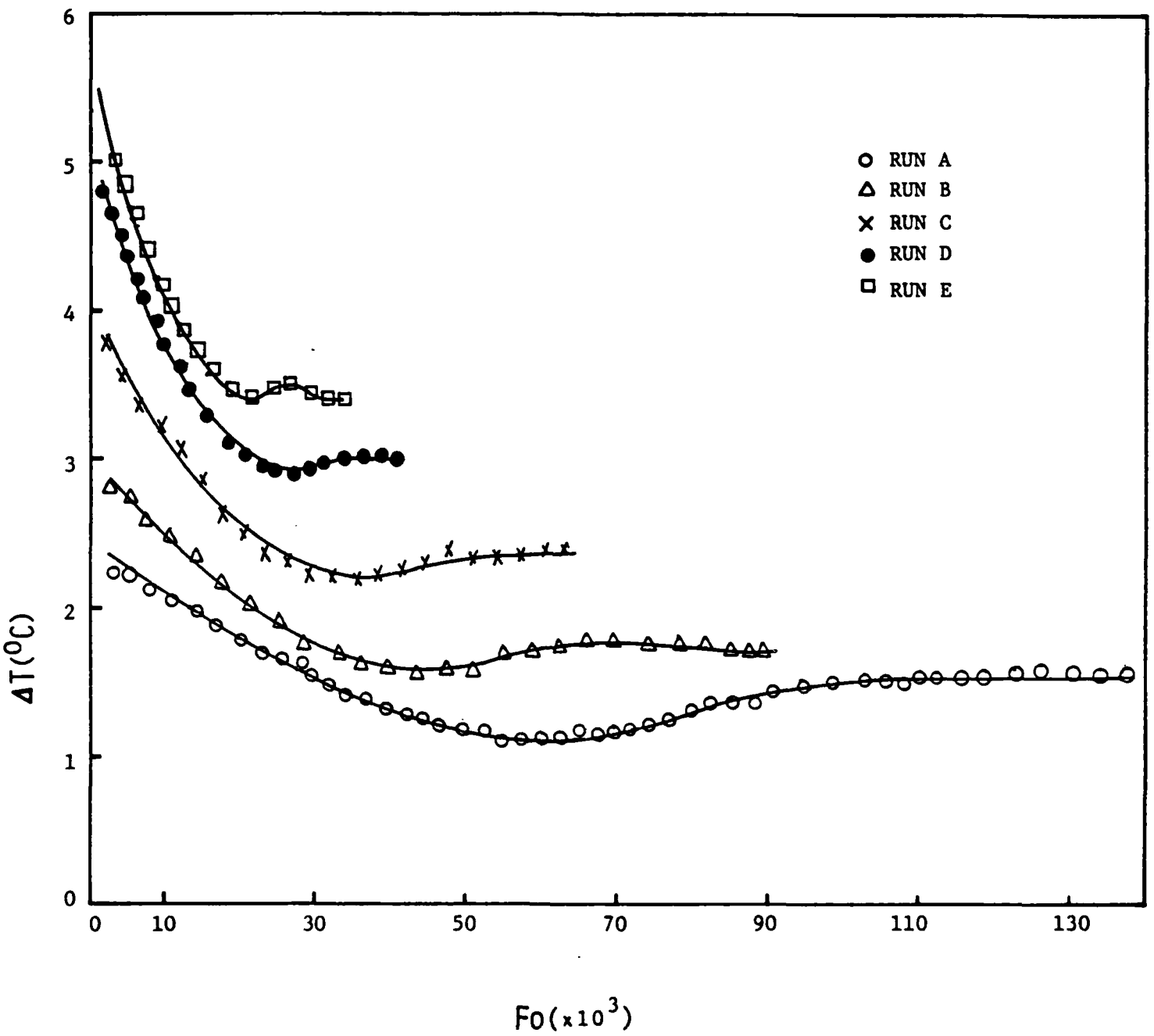


FIGURE 2.(a)

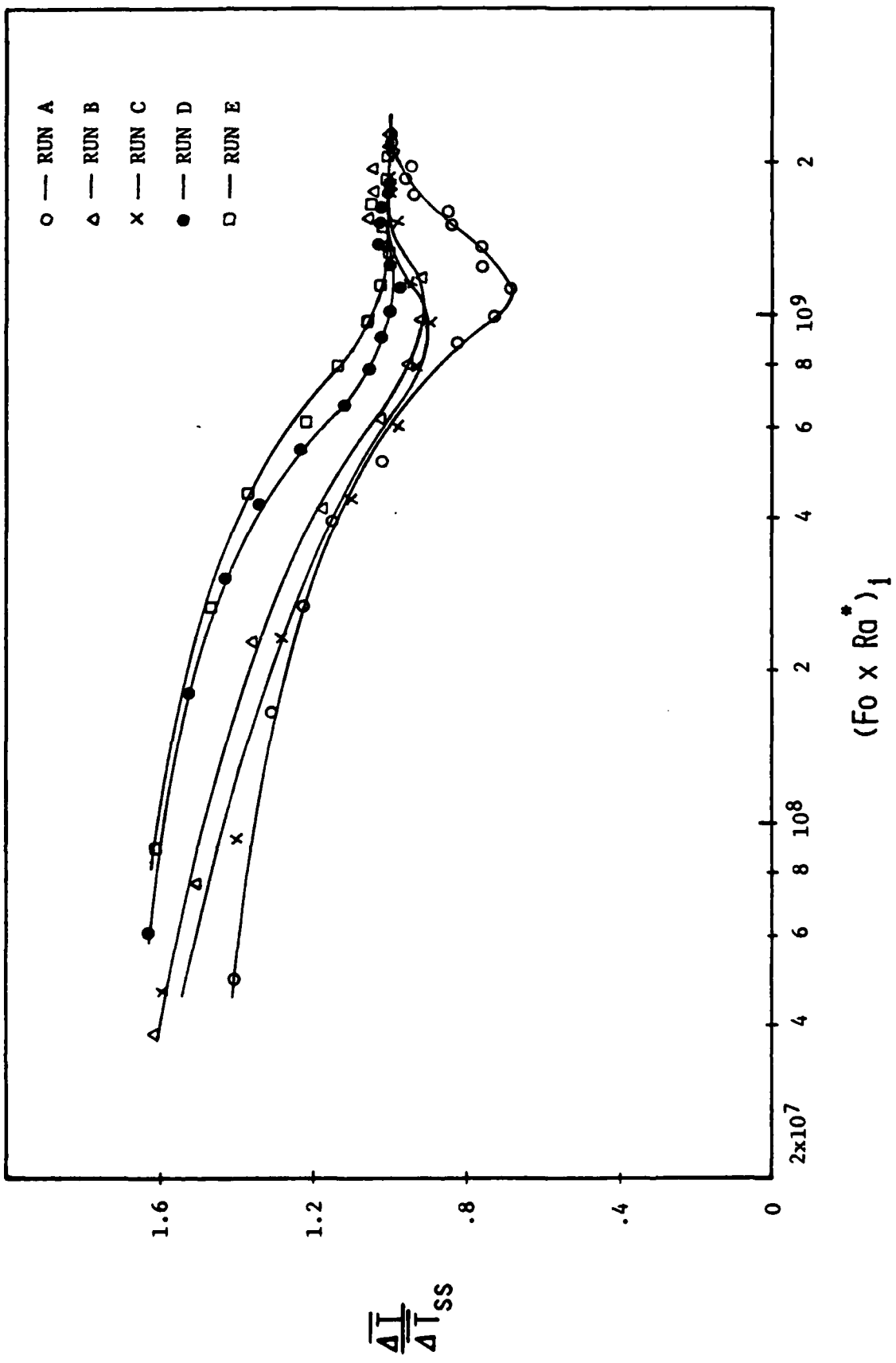


FIGURE 2.(b)

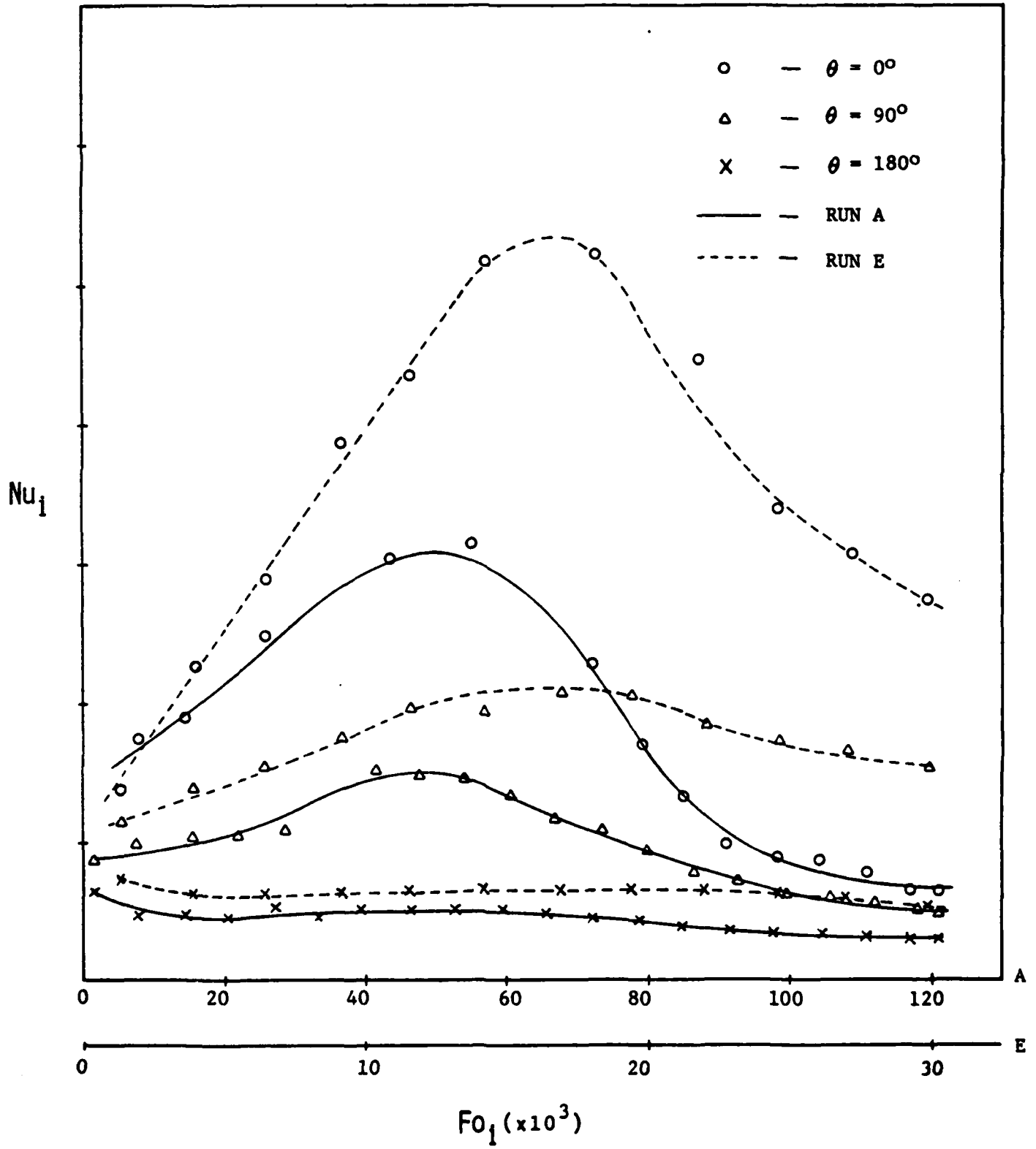


FIGURE 3

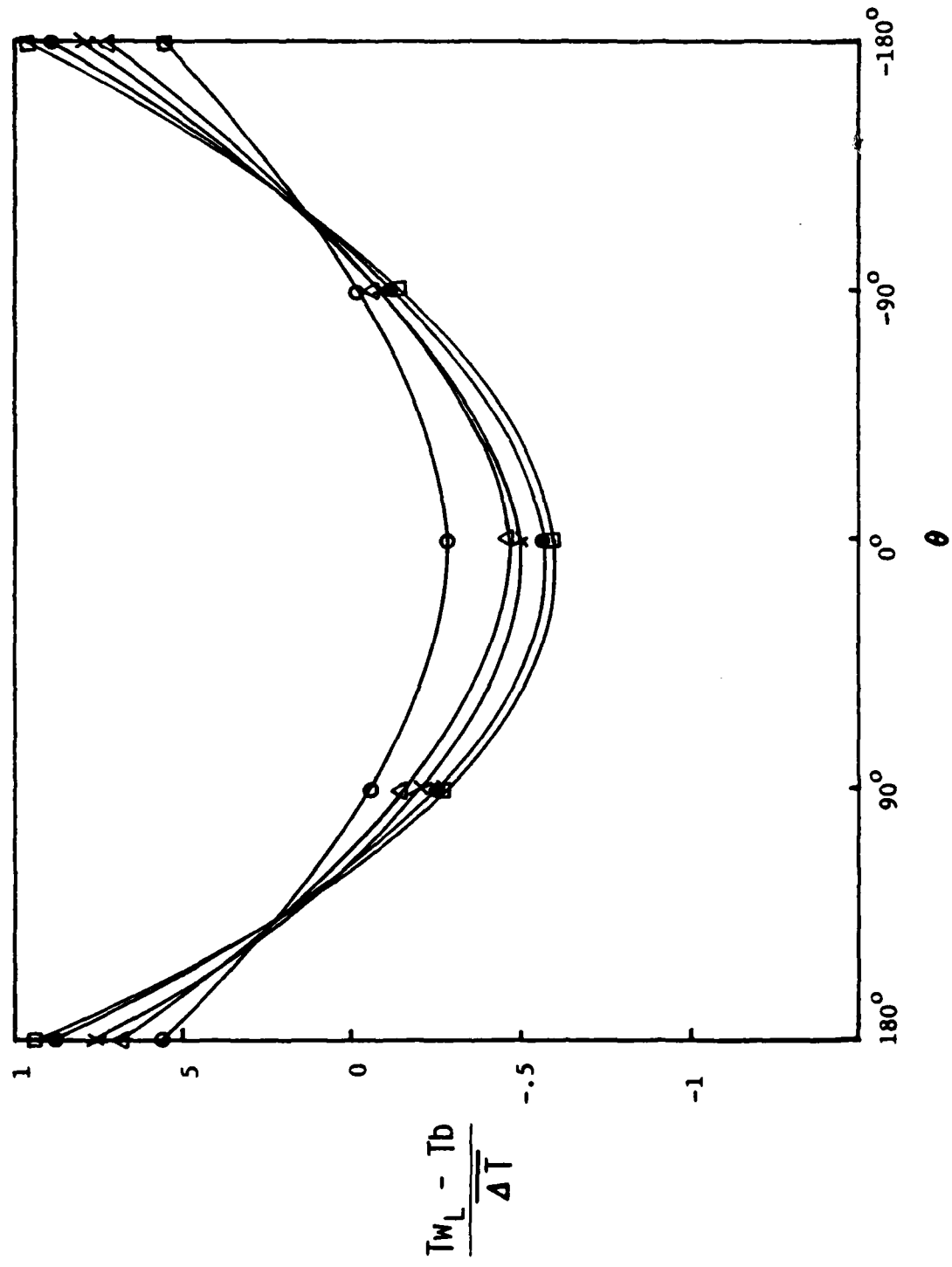


FIGURE 4

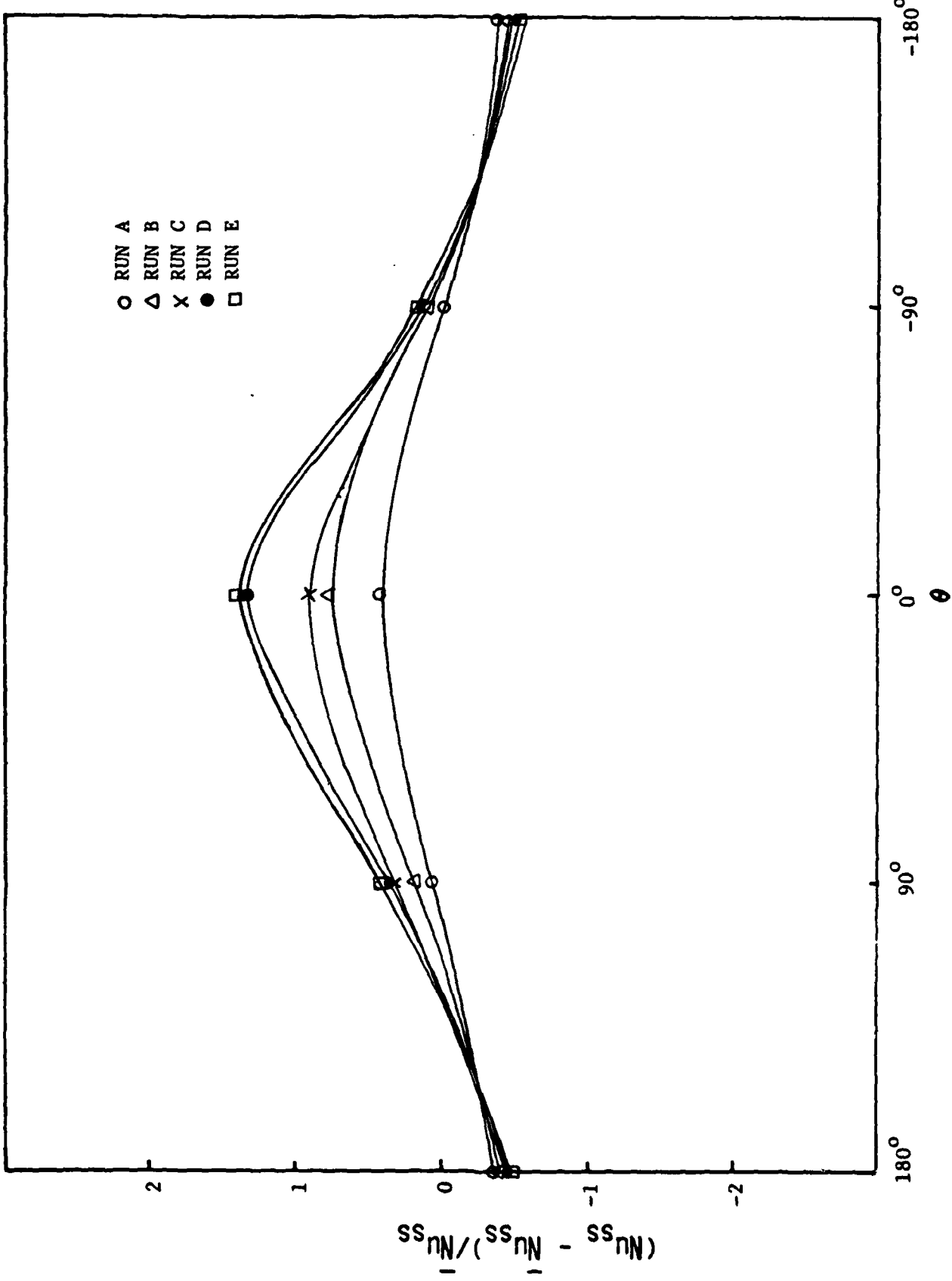


FIGURE 5

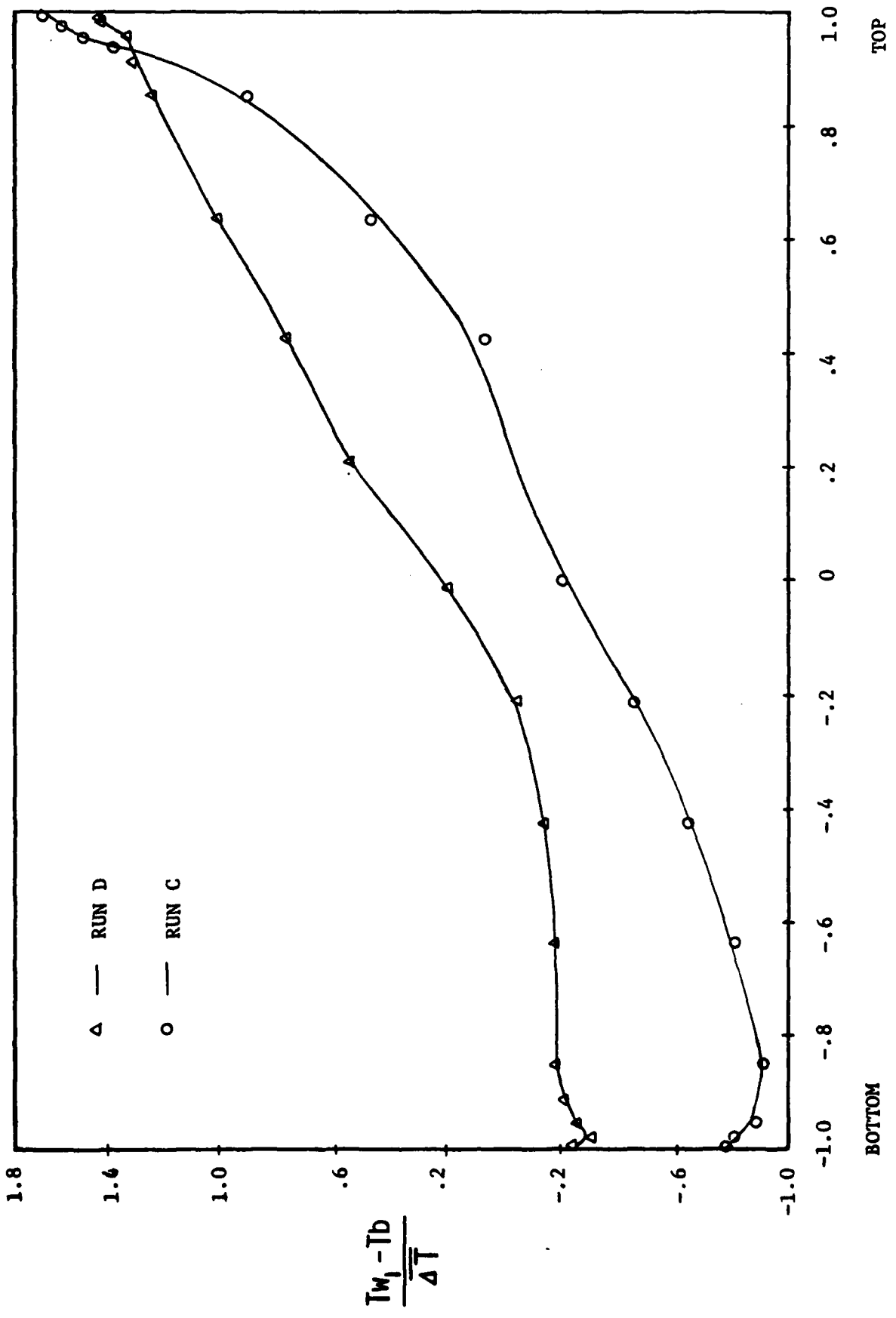


FIGURE 6(a)

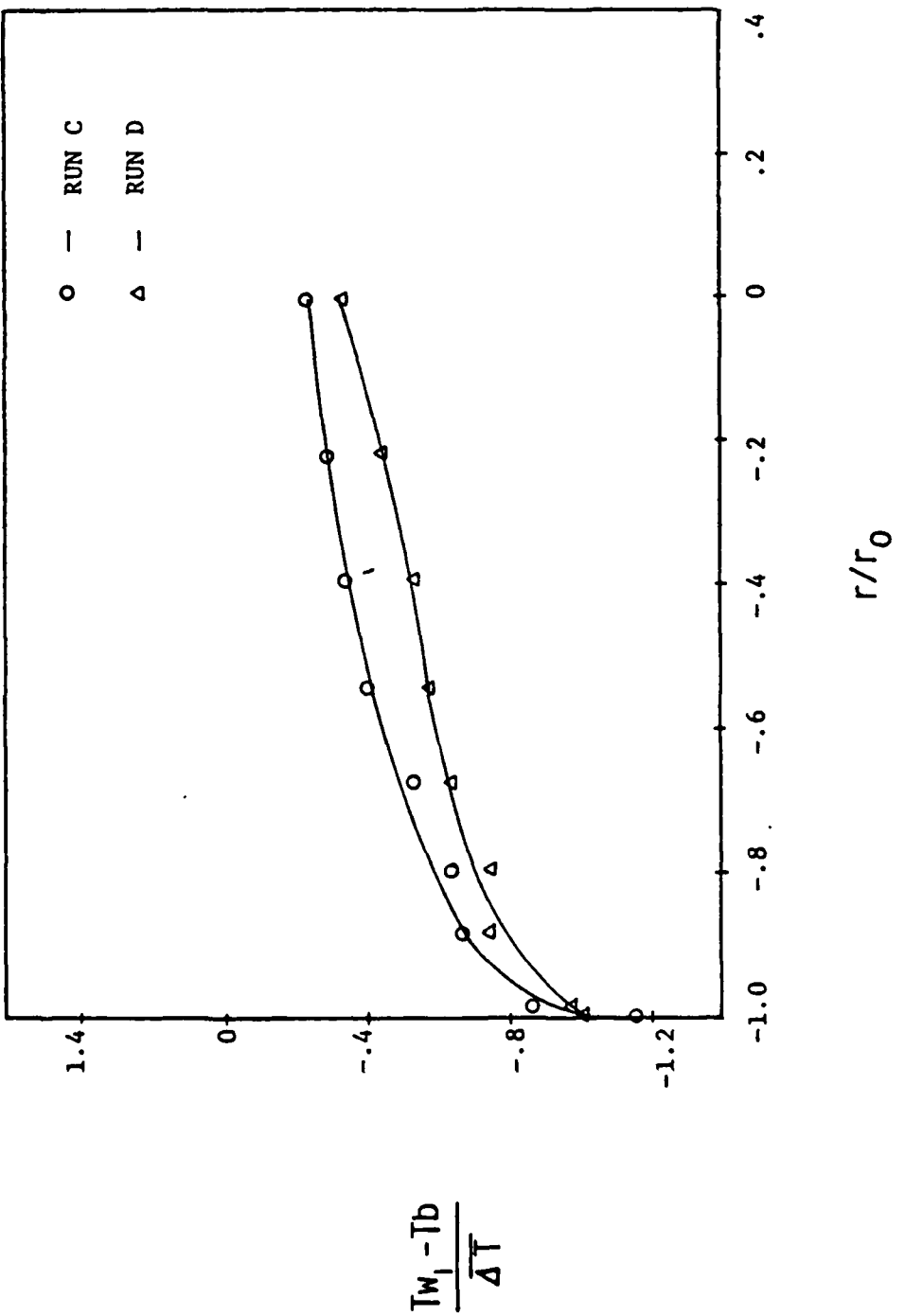


FIGURE 6.(b)

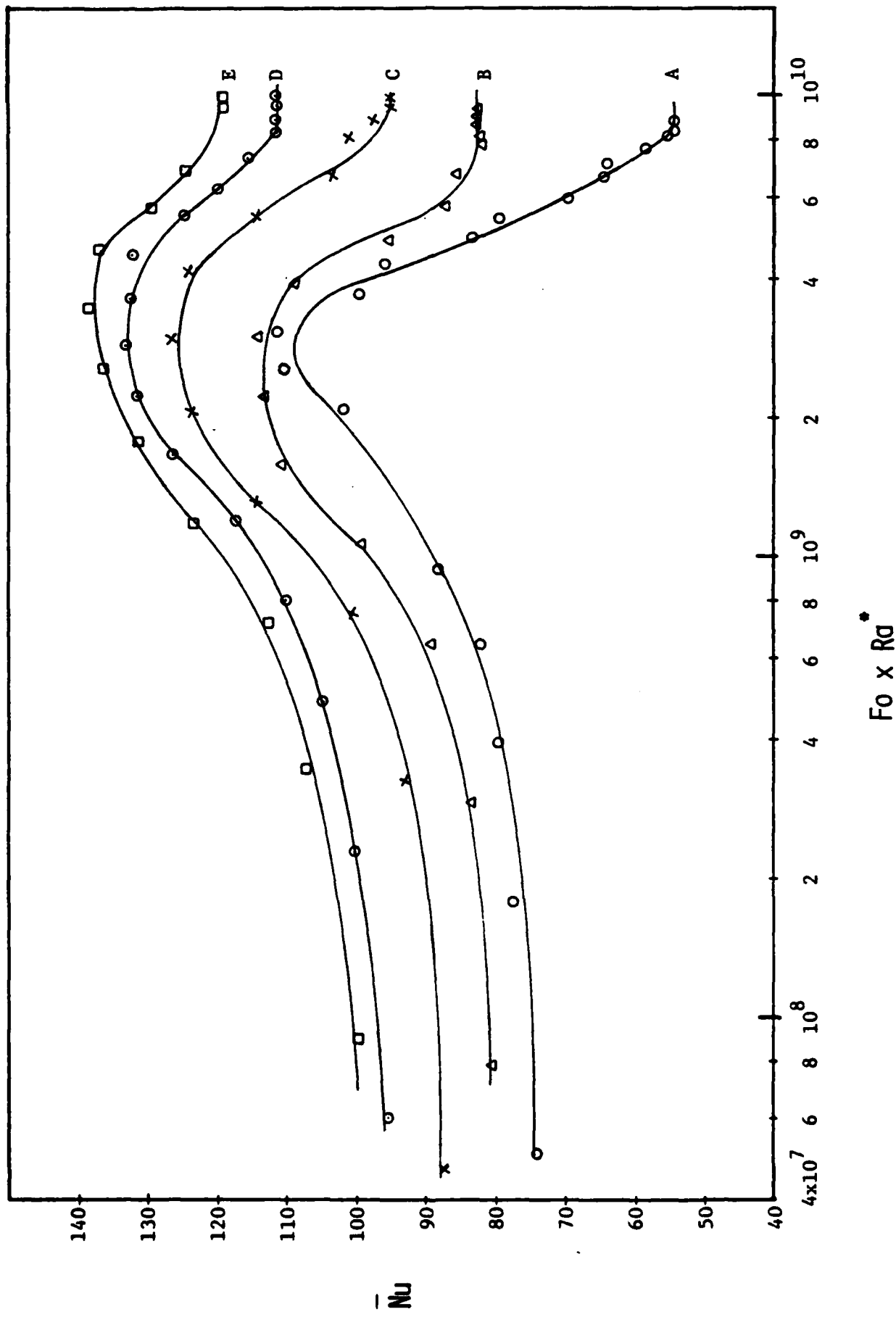


FIGURE 7. (a)

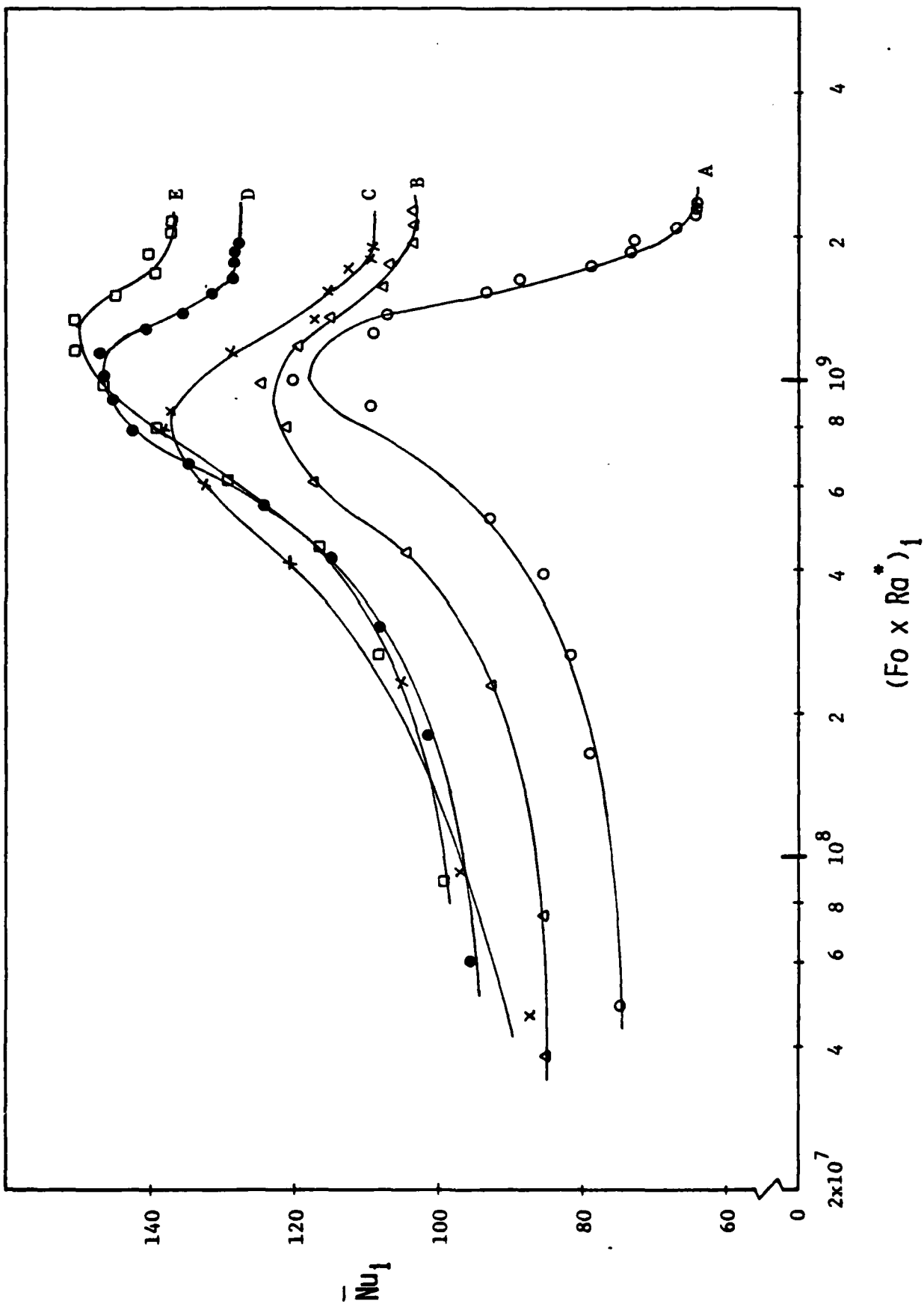


FIGURE 7 . (b)

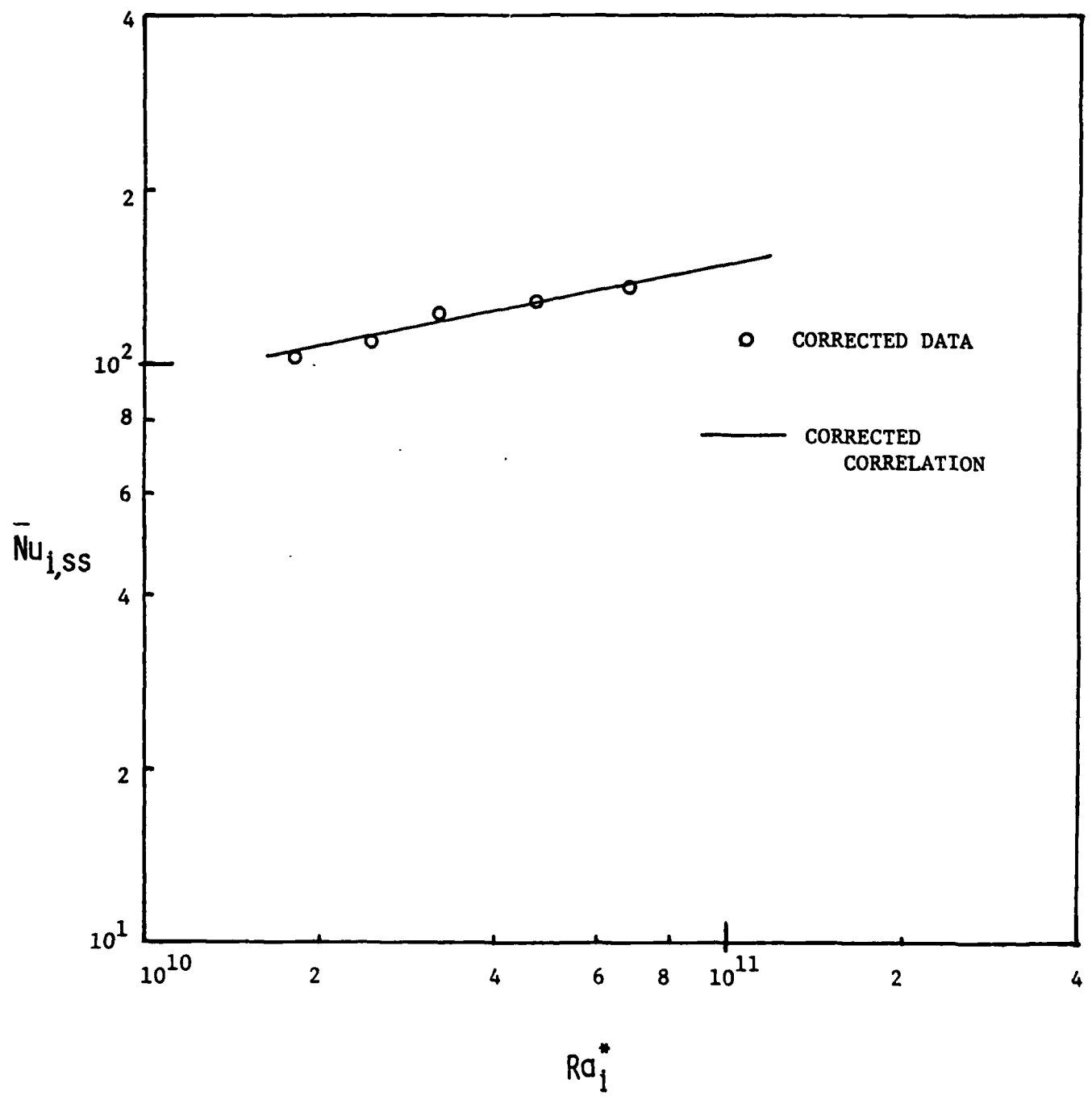


FIGURE 8

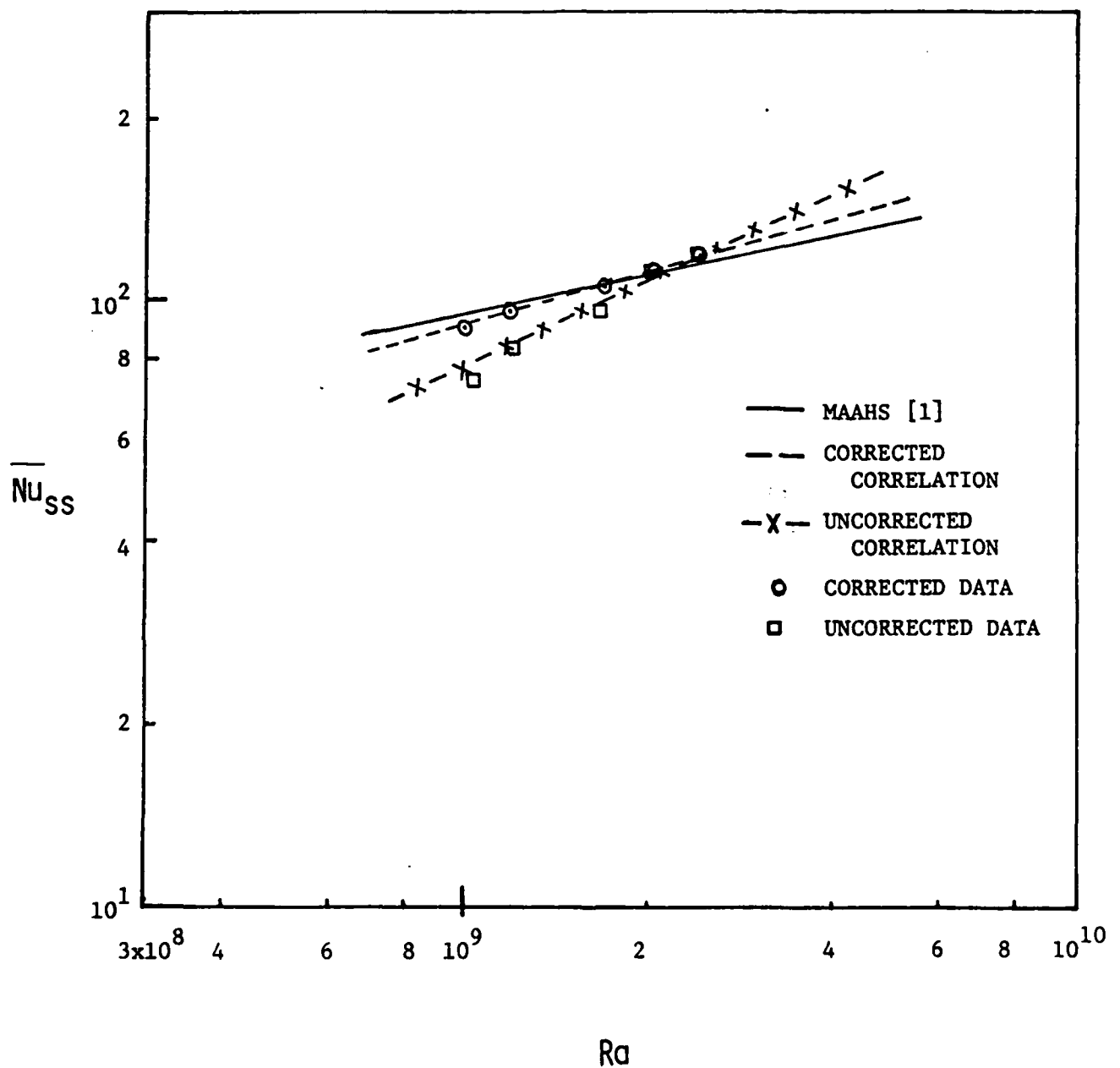


FIGURE 9

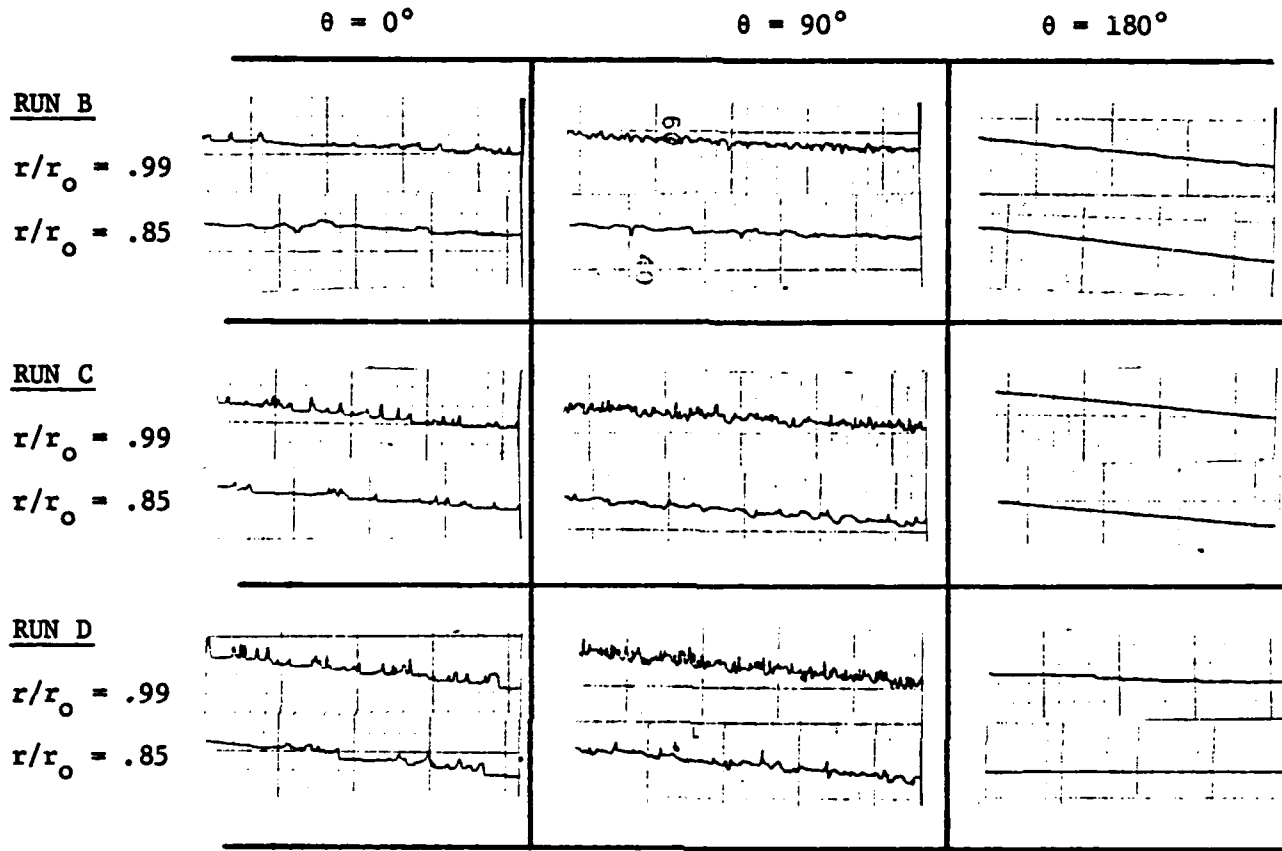


FIGURE 10

## UNCLASSIFIED

SECURITY CLASSIFICATION OF THIS PAGE (When Data Entered)

REPORT DOCUMENTATION PAGE		READ INSTRUCTIONS BEFORE COMPLETING FORM
1. REPORT NUMBER <b>AFOSR-TR- 82-0956</b>	2. GOVT ACCESSION NO. 10-4121-14	3. RECIPIENT'S CATALOG NUMBER
4. TITLE (and Subtitle) <b>INVESTIGATIONS OF TURBULENT NATURAL CONVECTION IN A HORIZONTAL CYLINDER</b>		5. TYPE OF REPORT & PERIOD COVERED <b>Final Report 1 May 80 - 15 May 82</b>
		6. PERFORMING ORG. REPORT NUMBER
7. AUTHOR(s) <b>James A. Liburdy</b>		8. CONTRACT OR GRANT NUMBER(s) <b>AFOSR-80-0181</b>
9. PERFORMING ORGANIZATION NAME AND ADDRESS <b>Mechanical Engineering Dept. Clemson University Clemson, SC 29631</b>		10. PROGRAM ELEMENT, PROJECT, TASK AREA & WORK UNIT NUMBERS <b>61102F 2307/A4</b>
11. CONTROLLING OFFICE NAME AND ADDRESS <b>AFOSR /NA Bolling Air Force Base, DC 20332</b>		12. REPORT DATE <b>July 82</b>
14. MONITORING AGENCY NAME & ADDRESS(if different from Controlling Office)		13. NUMBER OF PAGES <b>34</b>
		15. SECURITY CLASS. (of this report) <b>Unclassified</b>
		15a. DECLASSIFICATION/DOWNGRADING SCHEDULE
16. DISTRIBUTION STATEMENT (of this Report)  <b>Approved for Public Release; Distribution Unlimited.</b>		
17. DISTRIBUTION STATEMENT (of the abstract entered in Block 20, if different from Report)		
18. SUPPLEMENTARY NOTES  <b>Information contained in this report will be presented at the ASME 1982 Winter Annual Meeting, Nov. 1982, Phoenix, AZ</b>		
19. KEY WORDS (Continue on reverse side if necessary and identify by block number)  <b>Enclosure Natural Convection</b>		
20. ABSTRACT (Continue on reverse side if necessary and identify by block number)  <b>An experimental study examines the transient natural convective heat transfer in a liquid filled horizontal cylinder with a constant uniform heat flux. The transient and quasi-steady state response of the local and averaged Nusselt number is correlated with a modified Rayleigh number. The transient response is mapped against the stretch time scale represented by the product of the Fourier modulus and modified Rayleigh number. Internal fluid temperature probe measurements and flow visualization reveal boundary layer type flow</b>		

**UNCLASSIFIED**

SECURITY CLASSIFICATION OF THIS PAGE(When Data Entered)

along the side walls with increased temperature fluctuations near the wall. Unstable mixing zones occur near the top and bottom of the cylinder which may be three dimensional.

**UNCLASSIFIED**

SECURITY CLASSIFICATION OF THIS PAGE(When Data Ente